

Differences in the acoustic emission characteristics of rock salt compared with granite and marble during the damage evolution process

Zhaopeng Zhang^{1,2} · Ru Zhang^{1,2} · Heping Xie^{1,2} · Jianfeng Liu^{1,2} · Patrick Were³

Received: 30 December 2014 / Accepted: 4 April 2015 / Published online: 17 April 2015
© Springer-Verlag Berlin Heidelberg 2015

Abstract Rock salt cavities for energy storage are important elements of energy supply management and sustainability. The mechanical properties of other common rocks have already been adequately investigated, but a systematic characterization of the differences in acoustic emission (AE) characteristics among rock salt and other common rocks is needed. In this study, the AE characteristics of the full-regime uniaxial compression of rock salt and common rocks such as granite and marble were determined. A damage variable based on AE parameters and a methodology for its determination were established, including an analysis of the characteristics of the AE time-space evolution, the AE amplitude distribution and the damage evolution based on AE parameters. Clear differences were observed in the AE characteristics of rock salt compared with granite and marble during the damage evolution process. The AE activity and energy release of rock salt with coarse grains and nonuniform structures decreased gradually with increasing stress level. The AE activity of rock salt appeared in a continuous, group-occurring form. The AE spatial distribution of rock salt was relatively uniform, without a definite rupture surface. The AE amplitude distribution varied slowly, and the proportion of AE events with small amplitudes increased

gradually during compression in rock salt. Moreover, the damage in rock salt predominantly occurred during the pre-peak period, resulting in a large damage variable of 0.9 at peak stress. By contrast, the damage variables of granite and marble are only 0.5 and 0.1, respectively, at peak stress. Rock salt exhibited less damage when approaching failure, resulting in a gentler and steadier process. And the plastic characteristics of rock salt are relatively obvious. These properties, to some extent, ensure the safety of underground storage engineering when rock salt is chosen as the medium.

Keywords Rock salt · AE time-space evolution · AE amplitude · Damage variable

Introduction

Large underground cavities form once subsurface salt formations have been obtained through dissolution. As a well-behaved geologic body, rock salt has low permeability and creep behavior, which can ensure good sealing performance of underground cavities and greater adaptability to deformation. Such an underground space can provide a good reserve or disposal site for materials that do not dissolve in salt, such as underground energy, hydrocarbons such as petroleum and natural gas, and waste such as nuclear waste, poisonous rubbish and CO₂ (Hunsche and Hampel 1999; Lavrov et al. 2002). In several Western countries, rock salt is the main type of geological formation used for underground energy storage. Rock salt is considered an ideal medium for subsurface energy storage. Therefore, comprehensive studies on the mechanical and stability properties of rock salt are needed.

✉ Ru Zhang
zhangru@scu.edu.cn

¹ State Key Laboratory of Hydraulics and Mountain River Engineering, Sichuan University, Chengdu 610065, China

² College of Water Resource and Hydropower, Sichuan University, No. 24 South Section 1, Yihuan Road, 610065 Chengdu, China

³ Energy Research Centre Niedersachsen, Clausthal University of Technology, Clausthal-Zellerfeld, Germany

The construction and utilization of salt cavities and the properties of rock salt have already been extensively studied. In a study of the constitutive model of rock salt, Weidinger et al. (1997) conducted compression tests of rock salt in the laboratory and established a composite model of plastic deformation based on the microstructure of the rock and its deformation mechanism, thereby enabling the prediction of the creep behavior of rock salt. Studies have also investigated damage evolution, enabling the establishment of a dislocation slip theory of rock salt, a strength theory and an M-D constitutive model supported by field tests (Alkan et al. 2007; Munson 1997). Triaxial compression tests of rock salt, combined with measurements of gas permeability and wave velocity, have been conducted to explore the relationship between damage deformation and permeation (Popp et al. 2001; Schulze et al. 2001). Yang et al. (1999) conducted axial and triaxial creep tests of rock salt, while considering several influencing factors, such as the confining pressure and axial load, and proposed a relevant creep constitutive model. Hou (2003) analyzed the mechanical and hydraulic properties of rock salt in the excavation disturbance zone and established the Hou/Lux mathematical model. Hunsche and Hampel (1999) constructed a composite model based on micromechanics and verified that the model could adequately describe the deformation caused by stress and temperature and distinguish the creep behavior caused by the variation in impurity content of rock salt. In a study of the mechanical properties and factors that affect the stability of rock salt, Wang et al. (2011) simulated the stress states of an underground salt cavern used for the storage of oil and gas by applying a numerical method and discussed the deformation characteristics of rock salt in mud-containing strata. Xing et al. (2014) studied the mechanical and hydraulic properties of bedded rock salt based on laboratory tests. Systematic rock salt experiments at various loading rates have been designed to establish the effect of loading rate on the mechanical characteristics of rock salt (Lajtai et al. 1991; Liang et al. 2011). In a study of the stability of underground caverns, Shi et al. (2015) discussed the influence of filling abandoned salt caverns with alkali wastes on surface subsidence. Lee et al. (2011) and Shi et al. (2013) studied the outburst and flow laws of groundwater in an underground cavern and proposed an effective solution for ensuring the stability of underground caverns. In addition, several researchers have analyzed the stability of underground caverns based on damage theory (Ma et al. 2015; Zhang et al. 2014; Zhu and Wei 2011).

In contrast to other excavated caverns, rock salt caverns cannot be monitored and measured by entering the caverns. In addition, the conventional method of load and deformation monitoring can detect only the external information

(i.e., stress and strain) regarding the material under loading. Ultrasonic methods are useful evaluating the holistic variations in the material properties, but cannot precisely detect the evolution of damage and fractures in the material interior. However, the acoustic emission (AE) technique is a proper tool for studying the damage evolution process in rock salt caverns. An AE is defined as a transient elastic wave induced by the rapid release of energy within a material, and the AE signals that are spontaneously generated from the microcracking can provide information about the size, location and deformation mechanisms of these events as well as the properties of the medium through which the acoustic waves travel (Lockner 1993). Compared with conventional monitoring methods (i.e., the load and deformation monitoring method, the ultrasonic method), the AE technique enables continuous, real-time detection of the generation and development of microcracks in the interior of the material under loading and the identification of their positions and sizes. Therefore, the damage evolution of rock salt storage caverns that are in the process of development can be effectively monitored and analyzed using the AE technique. Significant progress has been made in the study of the AE characteristics of rock salt during the deformation and failure. Uniaxial compression tests have revealed that the loading conditions exert considerable influence on the AE characteristics of rock salt (Filimonov et al. 2002; Lavrov et al. 2002). Manthei (2005) explored the relationship between AE parameters and fracture in rock salt during the process of deformation and failure by triaxial compression tests. Xie et al. (2011) determined the evolution characteristics of the AE spatial fractal during the process of deformation and failure in uniaxial compression tests of layered rock salt. Menéndez and David (2013) analyzed the influence of environmental conditions on the weathering of porous rocks using the AE method. Although the above studies explored the mechanical properties and AE characteristics of rock salt during the deformation process using various methods, the characteristics of the AE temporal-spatial evolution during the damage evolution process of rock salt were not discussed systematically, particularly the differences in the AE characteristics of rock salt compared to other common rocks such as granite and marble. Therefore, this paper considers rock salt as the primary object of investigation and includes granite and marble as experimental materials for comparison to explore their differences. Based on the differences in their components and structures, full-regime uniaxial compression experiments to determine the AE characteristics of rock salt, granite and marble were performed using the MTS 815 rock mechanics testing system and the PCI-2 AE testing system. The AE temporal-spatial evolution characteristics, the AE amplitude distribution and the damage evolution characteristics were analyzed, and the differences in AE

characteristics of rock salt compared with granite and marble were explored. The results of this study will further the characterization of the deformation and failure process of rock salt, an optimal medium for underground energy storage, and will provide a reference for typical operations in underground energy storage engineering.

Experimental materials and methods

Specimen preparation

The experimental materials were rock salt and two types of hard rocks, i.e., granite and marble. The rock salt samples were obtained from the Jintan underground gas storage site in Jiangsu Province, China. The buried depth was approximately 1000–1200 m, and rock salt cores with diameters of 80–100 mm were extracted using the surface borehole method. Lathes and other equipment were used to accurately process the cylindrical surfaces and end faces of the rock salt specimens, to ensure their verticality, parallelism and smoothness. These specimens could not be processed into standard cylindrical samples because of the effects of deep core drilling, and the specimen length was less than twice their diameter. For comparison, Granite and marble samples were acquired from the Pubugou hydropower station in Sichuan Province, China, and a stone market, respectively. The rock cores were processed using several procedures, such as incision and polishing, and were then formed into standard cylindrical samples with $\Phi 50 \text{ mm} \times H100 \text{ mm}$. Two specimens of rock salt were prepared and numbered JT-M1 and JT-M2. Their average density and uniaxial compressive strength were 2.29 g/cm^3 and 21.67 MPa, respectively. Three specimens of granite were prepared and numbered Z1-7, Z1-8 and Z1-9. The average density and uniaxial compressive strength of these granite specimens were 2.61 g/cm^3 and 87.22 MPa, respectively. Similarly, three marble specimens numbered A7-1, A7-2 and A7-3 were prepared, and their average density and uniaxial compressive strength were 2.66 g/cm^3 and 79.42 MPa, respectively. The sample details are presented in Table 1.

The mineral constituents and structures of the rocks were as follows. The predominant mineral in Jintan rock salt was halite. The predominant mineral constituents of the investigated granite were quartz, potash feldspar, plagioclase and a small percentage of biotite. The investigated marble was pure white in color, and its predominant mineral was calcite, with some interior reflective crystals. These observations were acquired using a stereo-microscope, as shown in Fig. 1. The Jintan rock salt contained coarse crystalline grains, and its structure was extremely

nonuniform. The crystal arrangement in the rock salt was not compact and contained impurities such as mudstone and cement. The granite had an in-equigranular texture with medium-coarse grains. The mineral constituents and particle size distribution of the granite were uneven. Biotites appeared in an irregular flake or grained state, scattered between regions of quartz and feldspar. The marble contained a single mineral constituent, whose particles appeared to be quite fine, homogeneous and compactly arranged. The mineral constituents of the rock salt led to low strength but high ductility, with crystalline grains that were coarse and nonuniform compared to those of the granite and marble. These microstructural features provide a reference and micro-mechanical foundations for the analysis of the AE characteristics of rock salt presented later in this paper.

Testing equipment

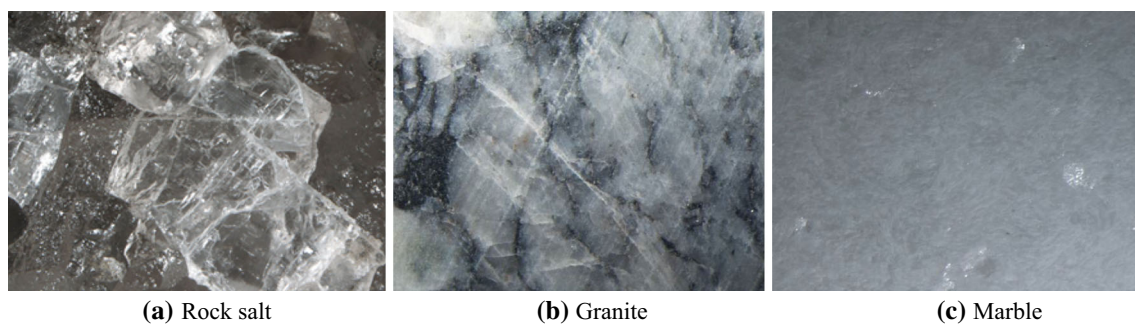
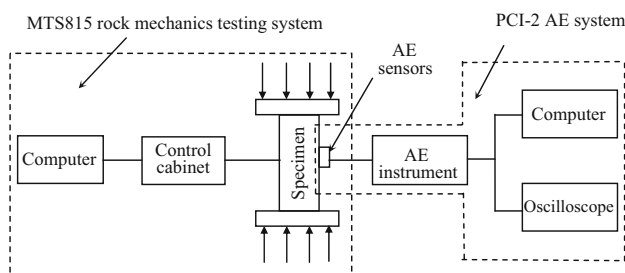
As shown in Fig. 2, the testing equipment was a combination of the MTS 815 Flex Test GT rock mechanics testing system and the PCI-2 AE system, with an 18-bit A/D and a bandwidth frequency of 1 kHz–3 MHz. The MTS 815 mechanical testing system is an automatic control system based on a digital computer, with a maximum axial loading capacity of 4600 kN, an axial displacement range of -50 to 50 mm, an axial/annular deformation extensometer with a measurement range of -4.0 to 4.0 mm and -2.5 to 12.5 mm, respectively. The simultaneous real-time monitoring of load, stress and displacement was performed during loading. Real-time AE characteristic parameter acquisition, waveform acquisition and analysis were performed simultaneously by the PCI-2 AE system, thereby enabling real-time AE monitoring and spatial orientation. The maximum signal amplitude was 100 dB, and the dynamic range was greater than 85 dB.

Testing method

Full-regime uniaxial compression tests of rock salt, granite and marble samples were conducted with real-time AE monitoring and positioning. Because of the large deformation and low strength of rock salt, axial displacement rate control was used for the rock salt specimens before peak loading, whereas for granite and marble, axial loading control was used prior to peak loading. The experimental setup for a sample is illustrated in Fig. 3. Eight individual AE sensors (1#–8#) were placed on the cylindrical surface of the sample using elastic bands; petroleum jelly was applied between the sample surface and the AE sensors to ensure perfect contact. Typical photographs of the samples before and after failure for all three rock types are

Table 1 Details of the specimens used in the test

Specimen number	Diameter (mm)	Length (mm)	Density (g/cm ³)	Young's modulus (GPa)	Poisson's ratio	Peak stress (MPa)	Axial strain corresponding to peak stress (%)	Rock type
JT-M1	75.07	91.92	2.33	20.63	0.15	20.02	1.31	Rock salt
JT-M2	72.49	103.31	2.24	17.91	0.15	24.49	2.74	
Z1-7	50.01	94.68	2.61	20.61	0.20	91.56	0.56	Granite
Z1-8	50.00	96.07	2.62	31.89	0.28	97.21	0.38	
Z1-9	50.02	99.29	2.60	24.55	0.19	72.88	0.34	
A7-1	49.48	105.33	2.66	27.96	0.35	79.98	0.33	Marble
A7-2	49.31	106.06	2.68	24.31	0.35	72.28	0.32	
A7-3	49.53	105.21	2.64	28.18	0.36	86.01	0.37	

**Fig. 1** Microscopic observations of the microstructures of the three rock types**Fig. 2** Schematic diagram of the testing system

presented in Fig. 4. To consider the effect of lithology, the test conditions (i.e., the experiment type, the arrangement of the AE sensors, the testing equipment and the test procedure) were identical for each rock type. Full-regime uniaxial compression tests and AE monitoring of the rock salt specimens were conducted, and the test results were compared with those for the granite and marble specimens. The AE temporal-spatial evolution characteristics, AE amplitude distribution and damage evolution based on AE parameters were analyzed to explore the differences in the AE characteristics of rock salt and those of granite and marble during the damage evolution process and the underlying mechanism.

Analysis of the test results

Differences and mechanism in the AE temporal-spatial evolution characteristics of rock salt compared with granite and marble

The AE time parameters used in this study included AE count, AE count rate, AE energy and AE energy rate. After all the specimens were tested, a typical specimen was selected to represent each rock type (i.e., JT-M2, Z1-8 and A7-1) and analyzed to compare AE time parameters and three-dimensional spatial distributions. The differences in the AE temporal-spatial evolution characteristics of the rock salt compared with granite and marble were determined, and the underlying mechanism was subsequently analyzed to explore the fundamental differences in the rock salt AE characteristics.

Differences in the AE time parameters of rock salt compared with granite and marble

The evolution curves of the AE time parameters and stress for the typical samples of rock salt, granite and marble are presented in Fig. 5. Compared with the common hard rocks

Fig. 3 Experimental setup for a test sample

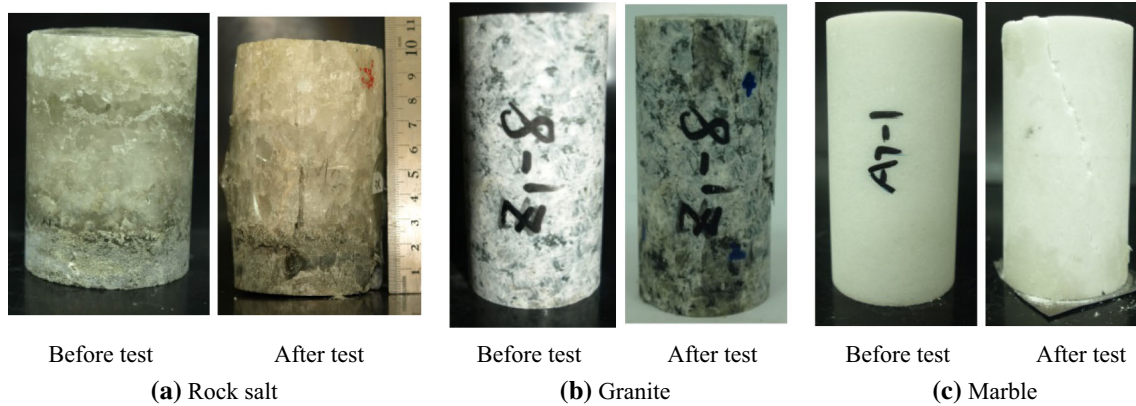
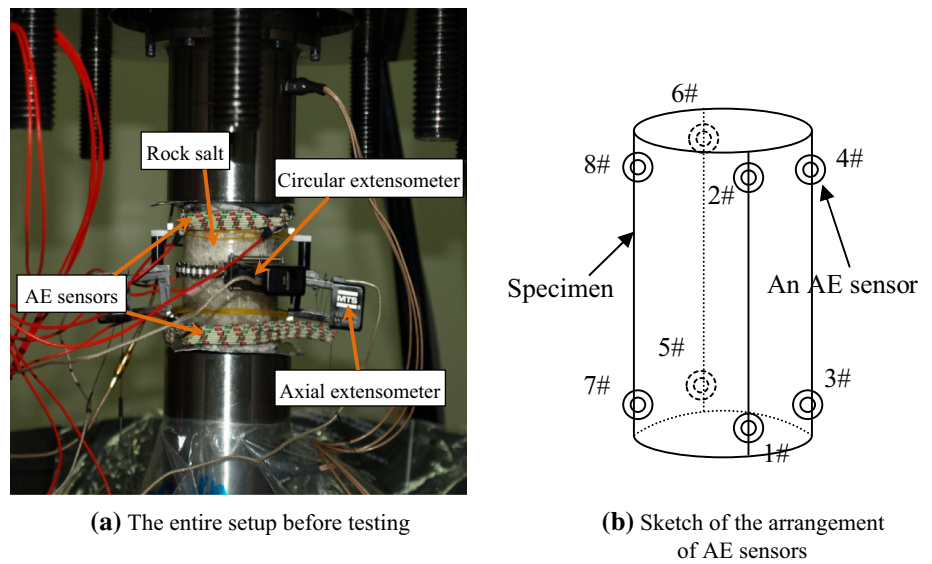


Fig. 4 Typical photographs of the three types of rock samples before and after failure

granite and marble, the rock salt exhibited clear differences in the evolution curves of AE time parameters and stress. Overall, the hard rock samples (i.e., granite and marble) exhibited a gradually increasing trend in the AE count rate and energy rate with increasing stress level prior to peak stress as the microcracks and energy release began to occur and gradually increased during the initial stages of loading. Prior to peak stress, peaks in AE count rates and energy rates predominantly appeared at stress levels of approximately 60–80 % in the granite and marble because a large number of microcracks and energy release occurred in this regime (see Fig. 5b₂₋₃, d₂₋₃). A transient AE quiet period occurred approaching peak stress in the granite and marble, but some microcracks and AE events were still generated after peak stress (see Fig. 5a₂₋₃, c₂₋₃). By contrast, for the rock salt, the AE count rate and energy rate exhibited peak levels during the early loading stage, and then gradually decreased with increasing stress level, with the value of AE energy rate remaining relatively high

throughout the entire loading process. This observation indicates that in the rock salt, massive microcracks and energy release were generated during the early stage of loading. Furthermore, very few microcracks or AE events were generated after peak stress. This profile implies that lithology has a significant effect on the evolutionary characteristics of the AE time parameters due to the differences in mineral constituents and structures. Compared with the granite and marble, the rock salt exhibited a distinct difference in the evolutionary characteristics of AE time parameters.

By analyzing the evolution curves of the AE count rates for the three types of rocks, marked differences in form were identified between the AE activity of the rock salt and that of the granite and marble. The form of the AE activity in the marble, which possessed fine grains and a uniform structure, was of the intermittent type, whereas in the rock salt, which exhibited coarse grains and a nonuniform structure, the form of the AE activity was of

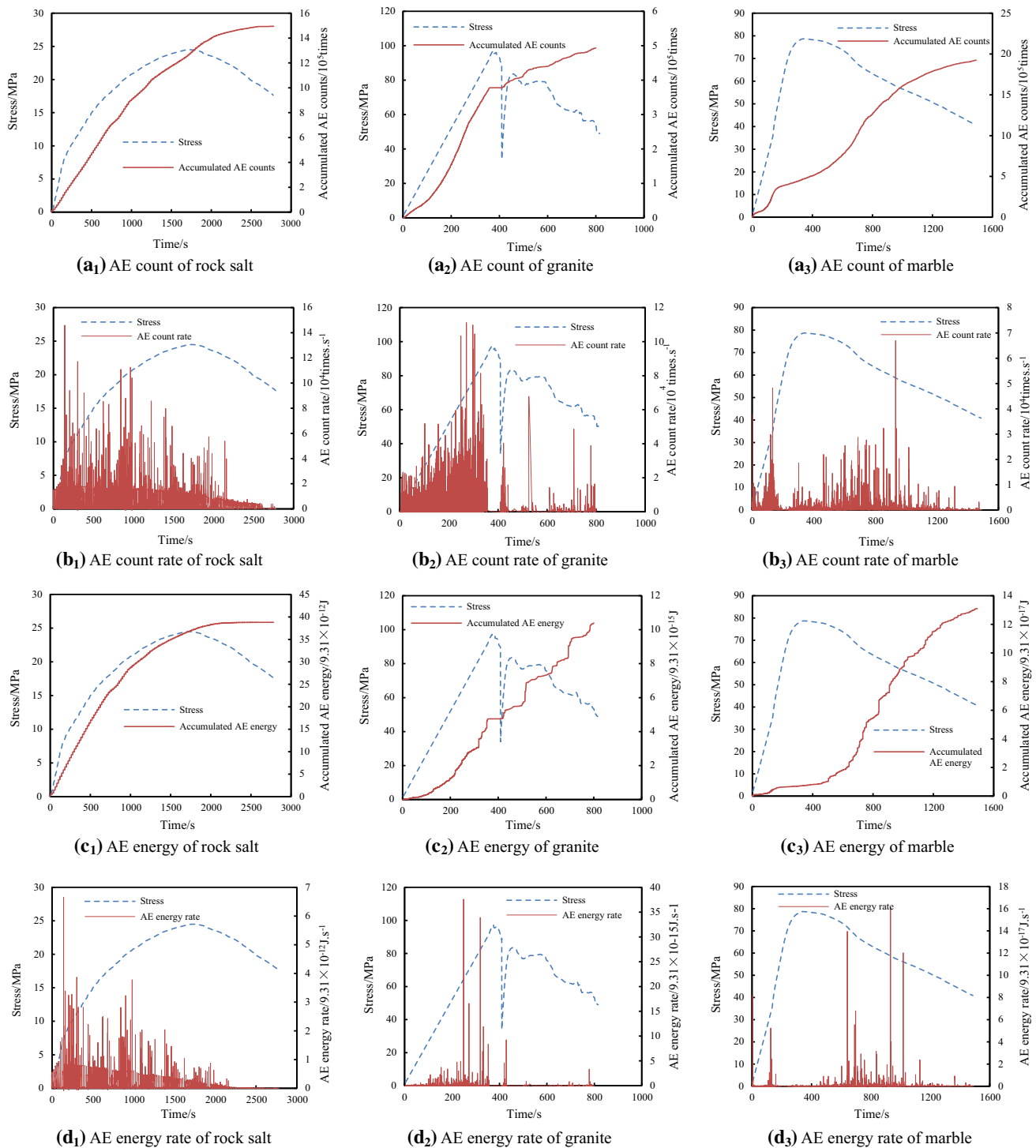


Fig. 5 Evolution curves of AE time parameters and stress over time for typical samples of rock salt (JT-M2), granite (Z1-8) and marble (A7-1)

the continuous type. The granite, which had medium-coarse grains and a nonuniform structure, exhibited an intermediate form of AE activity. Moreover, the AE events in the marble were weak overall, exhibiting a phenomenon of sudden bursts increasing from zero. By comparison, the AE events in the rock salt were relatively strong,

continuously generated, and rarely intermittent in form. Analyzing the evolution curves of the AE energy rates for the three types of rocks revealed that the AE energy released by granite and marble was rather sudden and intermittent in form. Whereas in the rock salt, AE energy was released in continuous form.

Differences in the AE spatial distribution of rock salt compared with granite and marble

Damage and fractures occur in rock under loading, and every location of an AE corresponds to a fracture in the rock during the process of deformation and failure. The AE spatial distribution reflects the characteristics of the spatial distribution of microcracks in the interior of the rock. Therefore, based on the characteristics of the AE three-dimensional location distribution, the differences in the AE spatial distribution of the rock salt compared with granite and marble can be inferred.

The AE spatial distributions corresponding to different stress-level intervals in the rock salt, granite and marble under uniaxial compression are shown in Fig. 6. In terms of the evolution of the AE spatial distribution, for the rock salt, the number of AE events gradually and continually increased and ultimately reached the maximum near peak stress. The AE spatial distributions in the granite and marble were very concentrated in space, with the obvious formation of a nucleation region. By comparison, the AE spatial distribution in the rock salt was relatively uniform, with AE event locations uniformly scattered in space without forming a distinct nucleation region.

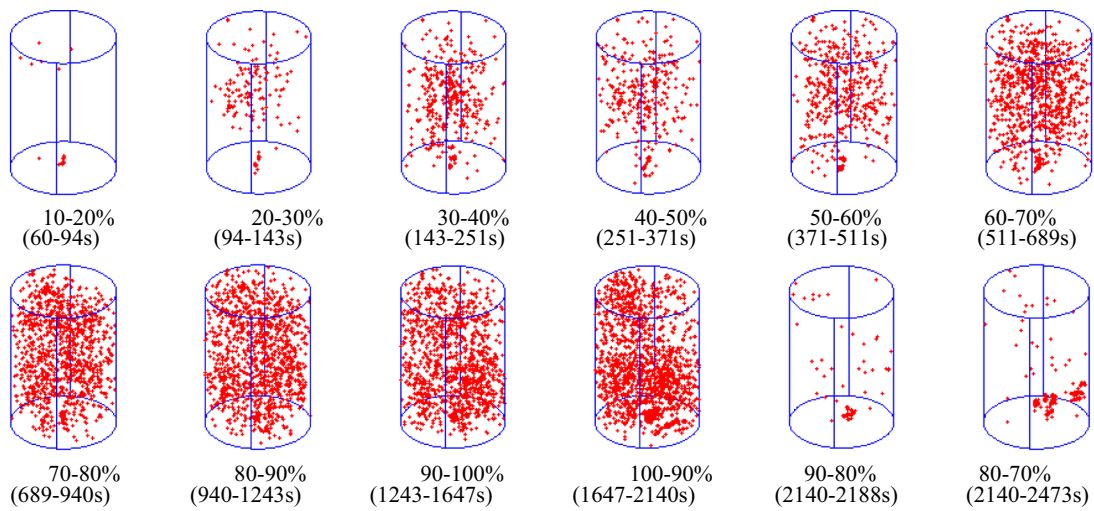
The patterns of the AE spatial distributions indicated that energy gradually accumulated in the granite and marble prior to peak loading and that a certain amount of accumulated energy then began to be released, leading to the production and development of microcracks in a specific region. Several major cracks rapidly extended and interconnected near peak stress, corresponding to intensive release of accumulated energy, as the bearing capacity of the granite or marble rapidly decreased. By contrast, in rock salt, microcracks were produced in a continuous and uniform fashion, and extended and interconnected slowly and in an orderly manner throughout the entire volume of the rock sample. The accumulated energy gradually dissipated during the deformation of the rock salt, without the formation of any major rupture. Finally, energy release occurred more smoothly and steadily during the process of failure; consequently, the bearing capacity of the rock salt slowly decreased. Thus, the failure process in the rock salt was relatively smooth compared with that in granite and marble, and sudden failure was rare. Consequently, rock salt can serve as an optimal medium for energy storage. The characteristics of rock salt are beneficial with regard to the safety precautions required in underground energy storage engineering.

The mechanism of AE characteristics differences of rock salt compared with granite and marble

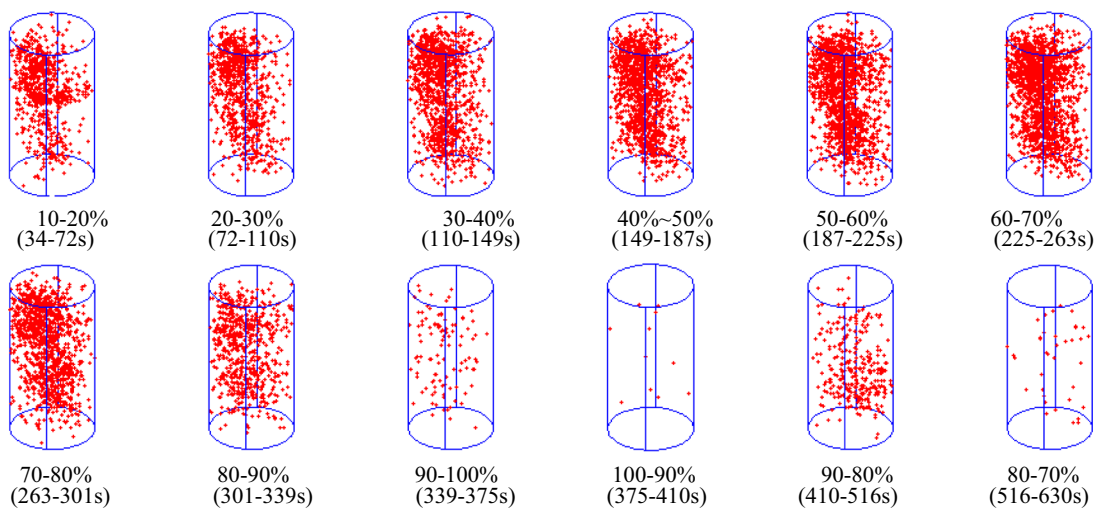
During the early loading stage, the granite and marble produced a lower AE count rate that then increased with

increasing stress level. By contrast, the number of AE counts produced in rock salt extremely high and rapidly reached peak during the early loading stage, then decreased with the increasing stress level. The constituents and structures of each rock type were analyzed to explain this phenomenon. In the granite and marble, the structures were compact, and the connection intensity between grains was relatively high. A certain number of microcracks will be produced, grow, nucleate and form macrocracks only once the stress level reaches a relatively high critical state. These properties led to the generation of a small amount of AE events during the early loading stage. As the stress level increases, the local stress state or deformation in the rock interior reaches the connection intensity or particles limit, and the AE counts then begin to increase gradually. By comparison, the grains of the rock salt were coarse, and the structures were nonuniform, with a relatively low connection intensity between grains. The AE activity predominantly originates from intergranular fractures, dislocation, slippage, crystal friction and the breakage of cement or sundries in the rock salt; such fractures are relatively easily generated during the early loading stage, leading to a high level of AE activity. However, as the damage evolution process progresses, self-resilience will cause the healing of partial defects and the closure of cracks during sustaining loading (Liang et al. 2007), and thus, the number of AE counts will gradually decrease as the stress level increases.

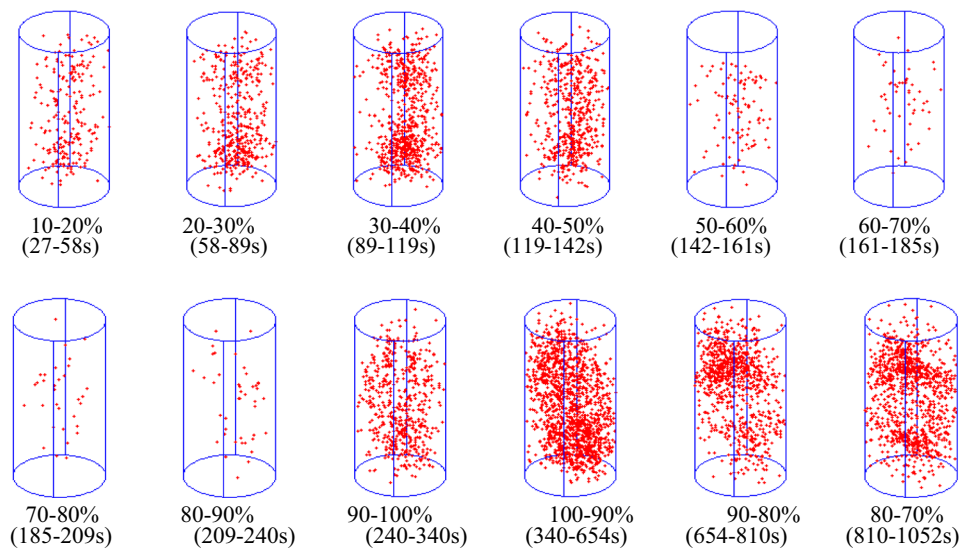
During the early loading stage, the granite and marble produce exhibited lower AE energy rate that then increased with increasing stress level. By comparison, the AE energy rate of the rock salt reached peak during the early loading stage and remained relatively high throughout the entire loading process. From the perspective of thermodynamics theory, the process of deformation and failure in rock is essentially an overall process of energy dissipation and energy release (Xie et al. 2005). Considering the axial strains corresponding to peak stress in Table 1 and the stress–time curves in Fig. 4, the brittleness of granite and marble was evident, their deformation was also quite small, and the majority of the energy absorbed from loading was stored as releasable elastic strain energy, which was consumed in the failure caused by macroscopic fractures. Conversely, the energy dissipation during the damage evolution remained relatively low throughout the entire process. By contrast, the plasticity of the rock salt was relatively obvious; its deformation was also quite large, and the majority of the energy absorbed from loading was converted into dissipation energy, which was consumed during the damage evolution process. Therefore, the AE energy rate reached the peak during the early stage and remained high throughout the entire process. Finally, the elastic strain energy that can be released during failure



(a) Rock salt



(b) Granite



(c) Marble

◀ **Fig. 6** AE spatial distributions corresponding to different stress-level intervals in the rock salt, granite and marble (100–90, 90–80 %, etc. represent stress-level intervals after peak stress)

caused by macroscopic fracturing was relatively small in the rock salt. To some extent, this explains why sudden and violent failure was rarely observed in the rock salt. In other words, in rock salt, the plastic deformation during the damage evolution consumed a massive amount of energy, and a relatively low amount of elastic strain energy accumulated for release during failure. Whereas the common hard rocks granite and marble accumulated more releasable elastic strain energy, which was then released more violently when failure occurred.

These differences can be explained in terms of the micromechanism of microcracks (Li 1995; Xie 1990). According to the dislocation pile-up model of Cottrell, microcracks or micropores will form only when the local stress σ_t satisfies Eq. (1).

$$\sigma_t \geq \frac{8\gamma G}{K_y} d^{-0.5} \tag{1}$$

where γ is the interface energy, d is the grain size, K_y is the yield constant, and G is the shear modulus.

Brittle fracture in a material begins to occur when the stable extension of microcrack turns into the unstable extension. The criterion for the brittle fracture is expressed by the following equation:

$$(\sigma_0 d^{0.5} + K_y) K_s \geq \beta G \gamma \tag{2}$$

where β is an ordinary constant and K_s is a constant that reflects the degree of dependence of the multicrystal yielding shear stress on $d^{0.5}$. σ_0 includes two components, one is related to the long-range stress provided by the macroscopic stress field, and the other originates from the crystal resistance and short-range stress of point defects. Equation (2) indicates that factors that cause σ_0 , K_y , K_s and d to increase can accelerate the brittle fracture of materials. Therefore, coarser rock grains and more nonuniform rock structures increase the likelihood that microcracks will form. For example, the rock salt had larger value of d and σ_0 compared to the granite and marble, indicating that its rock grains were larger and its rock structure was more nonuniform. In addition, a more nonuniform rock structure increases the discordance of the deformation between mineral grains, particularly in stress states with high local tension or pressure. Because the number of microcracks produced per unit time is higher in rock salt, the AE swarm phenomenon can readily occur. This mechanism effectively explains the characteristic pattern of AE activity observed during the loading of the rock salt.

Analysis of the differences in AE amplitude distribution of rock salt compared with granite and marble

The AE amplitude represents the maximum amplitude and strength of an AE event and is expressed in units of dB. Investigating the rules of the AE amplitude distribution in rock salt, granite and marble during the loading process could help reveal the differences in the AE amplitude distribution of rock salt compared with granite and marble and establish a deeper understanding of the evolutionary mechanism of deformation and failure.

In this paper, the characteristics of the AE amplitude distribution are described in terms of a parameter, whose value (the so-called b -value) represents the relationship between the magnitude and frequency of earthquakes and is usually used as an index of regional seismic activity. The logarithmic relationship between the magnitude and cumulative frequency of earthquakes is linear, with a slope equal to the b -value. Application of the b -value is not only limited to field of seismology. The AE events that occur in rock during the loading process can also be regarded as seismic activity (microseisms), and the law of the variation in the b -value for AE activity can be investigated during the deformation and failure of rock. The b -value can be calculated using the following equation:

$$\lg(N(A)) = C - b \lg(A) \tag{3}$$

where A is the AE amplitude during the loading process (dB), $N(A)$ is the number of AE events whose amplitudes are larger than A , C is a constant. The AE data from a test can be described using Eq. (3), and the b -values for each rock type in a given stress state are obtained by fitting the data to this equation in \lg – \lg coordinates. The b -value is the parameter of the AE amplitude distribution that represents the AE amplitude-frequency relationship. The b -value is also a parameter of the scale distribution of crack propagation and therefore represents the distribution of AE event magnitudes and the scale distribution of microcracks.

Previous research on the b -value (Colombo et al. 2003; Lockner 1993; Zeng and Ma 1995) has established three major results or rules. (1) An increase of the b -value implies a rise in the proportion of small AE events and the existence of predominantly small fractures, (2) invariance of the b -value indicates an invariant proportion in the distribution of AE event magnitudes and a fairly constant scale distribution of microcracks, (3) the decrease of the b -value means an increase in the proportion of AE events with large magnitude and an increase in the proportion of large fractures. Therefore, the b -value is used not only to represent the evolutionary characteristics of rock under different levels of stress during loading but also to compare the differences in the evolution of rock salt compared with

granite and marble under loading. According to Eq. (3), the b -values at different stress levels can be acquired from the statistics of the AE event amplitudes A and the number of AE events whose amplitudes are equal to or greater than the amplitude A at different stress levels.

Figure 7 shows the relationship curves of b vs. stress level for the rock salt, granite and marble. With regard to the trend of the variation of the b -value with stress level, the b -values of the granite and marble gradually decreased overall with increasing stress level. However, the b -value of rock salt exhibited an inverse trend, with a gradual, linear increase with increasing stress level. This finding reveals a clear difference between the AE amplitude distribution of rock salt and those of granite and marble. Generally, the law of the variation in the b -value reflects the characteristics of the variation in the AE amplitude distribution with stress level. In the granite and marble, as the stress level increased, the number of AE events with different amplitudes gradually increased, but the increase in the number of AE events with large amplitudes will be more pronounced than that of AE events with small amplitudes, resulting in an increase in the proportion of AE events with large amplitudes. The primary reason for this behavior is that the structures in the granite and marble are compact and the strength of their micro-units or the strength between micro-units is rather high; thus, their capacity to resist deformation and failure is quite high, and more energy can be accumulated in the rock before large microcracks form. As the stress level gradually reaches the energy release threshold, the accumulated energy begins to be released with high intensity, causing a rapid increase in the number of large microcracks as well as an increase in the number of AE events with large amplitudes. These increases result in a decreased b -value in the granite and marble. In the rock salt, however, as the stress level

increases, the increase in the number of AE events with small amplitudes is more pronounced than that of AE events with large amplitudes, resulting in an increase in the proportion of AE events with small amplitudes. The primary reason for this difference is that in the rock salt, the grains are quite coarse and the structure is not compact, and therefore, the strength of the micro-units or the strength between micro-units is rather low. As a result, it is quite difficult for a large amount of energy to accumulate and generate large microcracks in rock salt. However, it is easy for small microcracks to form and rapidly spread. This leads to an increased b -value in the rock salt.

As observed in Fig. 7, the b -value curves for granite and marble exhibit a wide range of variation and are not smooth but fluctuate violently, whereas the b -value curve for rock salt varies within a relatively small range and exhibits a smooth trend with little fluctuation. These observations indicate that the variation in the AE amplitude distribution during the loading process is more violent in granite and marble. The primary reason for this discrepancy is that the production and development of microcracks occur much more rapidly and suddenly during the loading process in hard rocks such as granite and marble, thereby causing sudden changes in the damage evolution process. By comparison, the variation in the AE amplitude distribution is much gentler and smoother in rock salt because the production and development of microcracks during the loading process are much smoother in rock salt and lead to a gradual and stable expansion process. In addition, as shown in Fig. 7, the b -value for rock salt is far lower than those for granite and marble at any given stress level, which also reflects the obvious difference in the AE amplitude distribution of rock salt compared with those of granite and marble. This observation indicates that under the same stress conditions, the proportion of AE events with large amplitudes (i.e., the proportion of large microcracks) will be much higher in rock salt than in granite or marble.

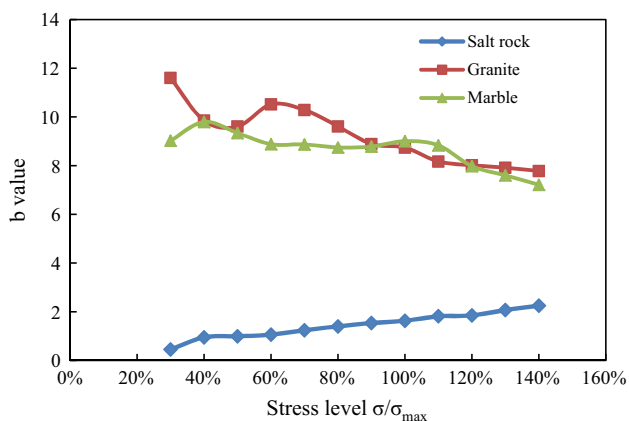


Fig. 7 Relationship curves of b vs. stress level for rock salt, granite and marble (the range of 110–140 % represents the post-peak stress-level range of 90–60 %)

Analysis of the differences in the damage evolution of rock salt based on AE parameters compared with granite and marble

When rock materials are subjected to load or temperature variation, a large amount of damage will occur in the interior of the rock. Microcracks or micropores will be produced, propagate and interconnect, resulting in the deterioration of the material's mechanical properties. During the damage evolution, the release of elastic strain energy, namely, the AE phenomenon, will occur. Therefore, AE activity and rock damage must be related such that the AE activity can indicate the degree of rock damage (Chen and Tang 1996; Rao and Lakshmi 2005). For this

reason, damage can be described not only by indirectly measuring the variations in the physical and mechanical properties of the material, as captured in a damage variable based on the variation in the elasticity modulus or the ultrasonic wave velocity, but also by applying the AE method. Therefore, this paper proposes the establishment of a damage variable based on AE parameters to explore the differences in damage evolution between rock salt and hard rocks such as granite and marble.

Based on the characteristic AE parameters discussed above, such as the AE count and AE energy, the damage variable can be established in accordance with the basic theory of damage mechanics. It is defined by the following equation (Ai et al. 2012; Zhang 2010):

$$D = \frac{N}{N_f} \tag{4}$$

where N_f represents the accumulated AE parameters when the rock sample is in a state of total failure and ΔA represents the accumulated AE parameters when the micro-unit ΔA is in the failure state. In this case, either the AE count or the AE energy could be used as the characteristic AE parameter. Current research on the damage evolution law of rock indicates that the AE energy is far more representative than the AE count of the real extent of damage in rock (Zhang 2010). Therefore, the damage variable based on the AE energy was adopted for the analysis presented in this paper. The relationship curves of the damage variable vs. the stress level for rock salt, granite and marble under uniaxial compression are presented in Fig. 8. The damage variable D based on the AE energy was calculated using Eq. (4).

As observed in Fig. 8, there is a marked difference between the damage evolution behavior of rock salt and that

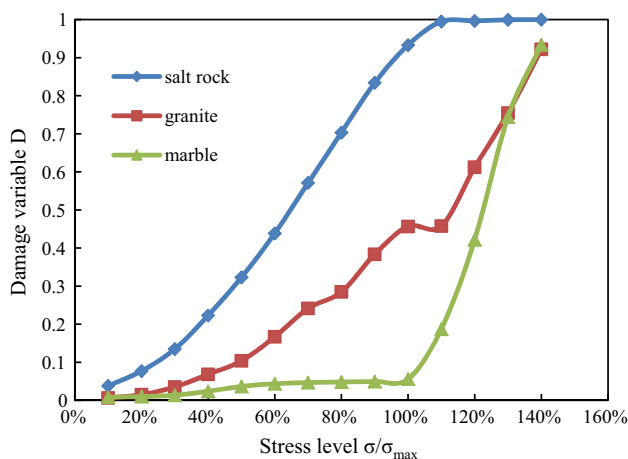


Fig. 8 Relationship curves of the damage variable vs. stress level for rock salt, granite and marble (the range of 110–140 % represents the post-peak stress-level range of 90–60 %)

of granite or marble. With increasing stress level, the damage variable curves for the three rock types trend from 0 to 1. At relatively low stress levels, the rate of increase in the damage variable is highest in rock salt, and the value of the damage variable reaches 0.9 at peak stress (i.e., 100 %). However, the damage variable in marble increases very slowly at low stress levels, attaining only a small value of less than 0.1 at peak stress. And subsequent loading after the peak stress will cause the trend in damage variable to change, and the value will abruptly increase to approach 1. The curve of damage variable for granite lies between those of rock salt and marble. The results indicate that the AE activity in marble remains at a low level during the early loading stage and that the damage remains minimal until the loading exceeds the peak stress. By comparison, the AE activity in rock salt is at a relatively high level during the early loading stage, causing massive damage to occur. The results also agree well with the analysis of the AE time parameters presented above.

The damage variables of rock salt, granite and marble are approximately 0.9, 0.5 and 0.1, respectively, at peak stress. These values indicate that during post-peak loading, the damage variables in rock salt, granite and marble increase by approximately 0.1, 0.5 and 0.9, respectively. The results imply that as failure approaches, the degree of damage in marble increases sharply, accompanied by massive damage and microcrack production. Consequently, a large number of AE events occur during this stage, and the failure process becomes more violent. This result, in combination with the stress–time curve for marble (Fig. 5a₃), confirms the obvious brittle nature of marble. By contrast, when approaching failure, rock salt exhibits a minimal increase in the degree of damage, as less damage and fewer microcracks are produced. Therefore, fewer or no AE events occur during this stage, and the failure process is much gentler. This result, in combination with the stress–time curve for rock salt (Fig. 5a₁), further confirms the obvious plastic nature of rock salt.

Conclusions

Through full-regime uniaxial compression experiments using rock salt, granite and marble, the AE time parameters, AE spatial parameters and AE amplitude parameters of these three rock types were acquired, and a method of establishing a damage variable based on AE parameters was proposed. Obvious differences were observed between the rock salt and other hard rocks such as marble and granite in terms of the AE time–space evolution, the AE amplitude distribution and the damage evolution based on AE parameters. Therefore, the main conclusions are as follows.

1. With regard to the evolutionary characteristics of the AE time parameters for rock salt, which contains coarse grains and nonuniform structures, the AE activity and energy release reach the peak during the early stage of loading. These parameters then begin to decrease gradually with increasing stress level, tending toward zero after peak stress is reached. In addition, the AE activity in rock salt appears in a continuous, group-occurring form. The plastic characteristics of rock salt are relatively obvious because the energy absorbed during loading is predominantly translated into dissipated energy, which is consumed throughout the entire damage process. The amount of accumulated strain energy that can then be released during the process of failure is smaller, and the failure process itself is much gentler. To some extent, these findings support the characterization of rock salt as an optimal medium for the underground storage of energy. The processes of deformation and failure in rock salt are relatively gentle and stable.
2. With regard to the evolutionary characteristics of the AE spatial distribution, the AE spatial distributions in granite and marble are concentrated in space, with the distinct formation of a nucleation zone in the interior of the rock. By comparison, the AE spatial distribution in rock salt is relatively uniform, without an obvious nucleation zone. No major ruptures form in rock salt, the energy release is much smoother and steadier, and the damage and intensity attenuation are relatively gentle.
3. With regard to the characteristics of the AE amplitude distribution, during the loading process in rock salt, the variation in the AE amplitude distribution is much gentler. In rock salt, as the stress level increases, the proportion of AE events with small amplitudes gradually increases, resulting in a corresponding increase in the *b*-value. The opposite result is observed in granite and marble. Moreover, the proportion of AE events with large amplitudes in rock salt is greater than that in granite or marble under the same stress conditions.
4. With regard to the characteristics of the damage evolution based on AE parameters, the damage in rock salt occurs predominantly during the early loading stage and gradually decreases with increasing stress level. These results are consistent with the law governing the evolution of the AE time parameters. The damage variable in granite and marble is 0.5 and 0.1, respectively, at peak stress. These values indicate that little damage is produced before peak stress, whereas massive damage occurs as failure approaches, resulting in a relatively violent process. The damage variable in rock salt is 0.9 at peak stress. This implies

that considerable damage occurs before peak stress and that little or minimal damage is produced when approaching failure, which is much gentler and steadier. This result further demonstrates the obvious plastic characteristics of rock salt. To some extent, the plastic nature of rock salt can ensure the safety of underground storage engineering when rock salt is chosen as the medium.

Acknowledgments This research was financially supported by the State Key Basic Research Program of China (No. 2011CB201201) and the National Natural Science Foundation of China (No. 51204113, 51120145001, 51134018).

References

- Ai T, Zhang R, Liu J, Ren L (2012) Space–time evolution rules of acoustic emission location of unloaded coal sample at different loading rates. *Int J Min Sci Tech* 22:847–854
- Alkan H, Cinar Y, Pusch G (2007) Rock salt dilatancy boundary from combined acoustic emission and triaxial compression tests. *Int J Rock Mech Min Sci* 44:108–119
- Chen Z, Tang C (1996) Effect of stiffness load on rock samples in AE test. *J China Coal Soc* 21:364–369 (in Chinese)
- Colombo IS, Main I, Forde M (2003) Assessing damage of reinforced concrete beam using “*b*-value” analysis of acoustic emission signals. *J Mater Civ Eng* 15:280–286
- Filimonov Y, Lavrov A, Shkuratnik V (2002) Acoustic emission in rock salt: effect of loading rate. *Strain* 38:157–159
- Hou Z (2003) Mechanical and hydraulic behavior of rock salt in the excavation disturbed zone around underground facilities. *Int J Rock Mech Min Sci* 40:725–738
- Hunsche U, Hampel A (1999) Rock salt—the mechanical properties of the host rock material for a radioactive waste repository. *Eng Geol* 52:271–291
- Lajtai E, Duncan ES, Carter B (1991) The effect of strain rate on rock strength. *Rock Mech Rock Eng* 24:99–109
- Lavrov A, Vervoort A, Filimonov Y, Wevers M, Mertens J (2002) Acoustic emission in host-rock material for radioactive waste disposal: comparison between clay and rock salt. *Bull Eng Geol Environ* 61:379–387
- Lee J, Jung B, Kim J-M, Ko K-S, Chang H-W (2011) Determination of groundwater flow regimes in underground storage caverns using tritium and helium isotopes. *Environ Earth Sci* 63:763–770
- Li L (1995) Characteristics of acoustic emission of rock. *Ind Miner Process* 24:37–40 (in Chinese)
- Liang WG, Yang CH, Zhao YS, Dusseault M, Liu J (2007) Experimental investigation of mechanical properties of bedded salt rock. *Int J Rock Mech Min Sci* 44:400–411
- Liang W, Zhao Y, Xu S, Dusseault M (2011) Effect of strain rate on the mechanical properties of salt rock. *Int J Rock Mech Min Sci* 48:161–167
- Lockner D (1993) The role of acoustic emission in the study of rock fracture. *Int J Rock Mech Min Sci Geomech Abstr* 7:883–899
- Ma H, Yang C, Li Y, Shi X, Liu J, Wang T (2015) Stability evaluation of the underground gas storage in rock salts based on new partitions of the surrounding rock. *Environ Earth Sci*. doi:10.1007/s12665-015-4019-1
- Manthei G (2005) Characterization of acoustic emission sources in a rock salt specimen under triaxial compression. *Bull Seismol Soc Am* 95:1674–1700

- Menéndez B, David C (2013) The influence of environmental conditions on weathering of porous rocks by gypsum: a non-destructive study using acoustic emissions. *Environ Earth Sci* 68:1691–1706
- Munson D (1997) Constitutive model of creep in rock salt applied to underground room closure. *Int J Rock Mech Min Sci* 34:233–247
- Popp T, Kern H, Schulze O (2001) Evolution of dilatancy and permeability in rock salt during hydrostatic compaction and triaxial deformation. *J Geophys Res Solid Earth* (1978–2012) 106:4061–4078
- Rao M, Lakshmi KP (2005) Analysis of *b*-value and improved *b*-value of acoustic emissions accompanying rock. *Curr Sci* 89
- Schulze O, Popp T, Kern H (2001) Development of damage and permeability in deforming rock salt. *Eng Geol* 61:163–180
- Shi T, Chen Z, Luo Z, Wang S, Wang K (2013) Mechanism of groundwater bursting in a deep rock salt mine region: a case study of the Anpeng trona and glauber mines, China. *Environ Earth Sci* 68:229–239
- Shi X, Li Y, Yang C, Xu Y, Ma H, Liu W, Ji G (2015) Influences of filling abandoned salt caverns with alkali wastes on surface subsidence. *Environ Earth Sci* 1–12
- Wang G, Guo K, Christianson M, Konietzky H (2011) Deformation characteristics of rock salt with mudstone interbeds surrounding gas and oil storage cavern. *Int J Rock Mech Min Sci* 48:871–877
- Weidinger P, Hampel A, Blum W, Hunsche U (1997) Creep behaviour of natural rock salt and its description with the composite model. *Mater Sci Eng, A* 234:646–648
- Xie H (1990) Damage mechanics of rock and concrete. Press of Chinese University of Minerals, pp 205–215
- Xie H, Peng R, Ju Y, Zhou H (2005) On energy analysis of rock failure. *J Rock Mech Eng* 24:2603–2608 (in Chinese)
- Xie H, Liu J, Ju Y, Li J, Xie L (2011) Fractal property of spatial distribution of acoustic emissions during the failure process of bedded rock salt. *Int J Rock Mech Min Sci* 48:1344–1351
- Xing W, Zhao J, Düsterloh U, Brückner D, Hou Z, Xie L, Liu J (2014) Experimental study of mechanical and hydraulic properties of bedded rock salt from the Jintan location. *Acta Geotech* 9:145–151
- Yang C, Daemen J, Yin J-H (1999) Experimental investigation of creep behavior of salt rock. *Int J Rock Mech Min Sci* 36:233–242
- Zeng Z, Ma J (1995) AE *b*-value dynamic features during rockmass fracturing and their significances. *Seismol Geol* 17:7–12 (in Chinese)
- Zhang R (2010) Research on AE properties of rock damage evolution process and rockburst integrated prediction. Sichuan University, Chengdu
- Zhang C, Feng X-T, Zhou H, Qiu S, Yang Y (2014) Rock mass damage induced by rockbursts occurring on tunnel floors: a case study of two tunnels at the Jinping II Hydropower Station. *Environ Earth Sci* 71:441–450
- Zhu W, Wei C (2011) Numerical simulation on mining-induced water inrushes related to geologic structures using a damage-based hydromechanical model. *Environ Earth Sci* 62:43–54